Editors' Suggestion

High-Power Collective Charging of a Solid-State Quantum Battery

Dario Ferraro,[1,*] Michele Campisi,[1] Gian Marcello Andolina,[1,2] Vittorio Pellegrini,[1] and Marco Polini[1]
[1]Istituto Italiano di Tecnologia, Graphene Labs, Via Morego 30, I-16163 Genova, Italy
[2]NEST, Scuola Normale Superiore, I-56126 Pisa, Italy

(Received 31 October 2017; published 15 March 2018)

Quantum information theorems state that it is possible to exploit collective quantum resources to greatly enhance the charging power of quantum batteries (QBs) made of many identical elementary units. We here present and solve a model of a QB that can be engineered in solid-state architectures. It consists of N two-level systems coupled to a single photonic mode in a cavity. We contrast this collective model ("Dicke QB"), whereby entanglement is genuinely created by the common photonic mode, to the one in which each two-level system is coupled to its own separate cavity mode ("Rabi QB"). By employing exact diagonalization, we demonstrate the emergence of a quantum advantage in the charging power of Dicke QBs, which scales like $\sqrt{N}$ for $N \gg 1$.

DOI: 10.1103/PhysRevLett.120.117702

Introduction.—In the last few decades, batteries [1,2] have been the driving force behind the revolution in personal electronics and, more recently, in the automotive sector [3]. Currently, there is also an ever-increasing demand on energy storage systems able to manage large power densities [4], an issue that has been so far partially addressed by the use of supercapacitors [5,6]. Batteries and supercapacitors essentially operate on the basis of robust electrochemical principles developed between the 18th and 19th centuries [1,2]. While it is pivotal to continue research on advanced materials [7] to optimize the performance of available energy storage devices, it seems timely to ask ourselves whether it is useful to transcend conventional electrochemistry to create an entirely new class of powerful batteries.

Quantum phenomena, such as phase coherence and entanglement, constitute remarkable resources that may enable superior performance of future technological devices. The prime example is quantum computing performed with quantum bits (realized, e.g., with superconducting circuitry [8,9]) as compared to classical computing performed with classical bits [10]. While in quantum computing quantum phenomena are employed to achieve efficient manipulation and processing of information, an emerging theoretical research activity is currently focused on utilizing genuine quantum resources to achieve superior performances in the manipulation and processing of energy [11–20].

Given this context, we are naturally led to consider whether quantum resources may be employed to improve the performance (e.g., by speeding up the charging time) of "quantum batteries" (QBs). To this end, we consider a quantum system—see red box in Fig. 1(a)—having a discrete energy spectrum, which can be kept well isolated from its environment so as to hold its energy for a sufficiently long time relative to the intended use. Many of such systems can be considered together, making a QB. In Figs. 1(a) and 1(b) we see two examples. In Fig. 1(a), each quantum system—in this case a two-level system (TLS)—is coupled to a separate cavity, each hosting a single photonic mode. In Fig. 1(b), an ensemble of many TLSs is embedded in a single cavity and interacting with a common photonic mode. Charging of a QB requires a protocol of "interaction" of the QB itself with some external body or field (the "energy source," namely, the

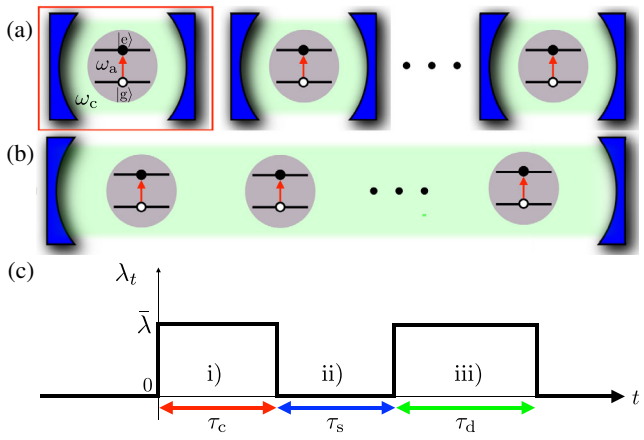

FIG. 1. (a) An array of identical Rabi quantum batteries operating in parallel. The elementary building block (red box), consists of a two-level system with an energy separation $\hbar\omega_a$ between the ground $|g\rangle$ and excited state $|e\rangle$. Each two-level system is coupled to a separate photonic cavity (blue). The red arrow indicates a particle-hole transition induced by the photon field. (b) A Dicke quantum battery, where the same array of two-level systems is now embedded into a single cavity and interacting with a common photonic mode. (c) Charging, storage, and discharging protocol, as described in the text.

cavity field in our example), which raises its energy over a timespan that is much shorter than the QB lifetime.

Early pioneering works [21–24] have considered a special subclass of charging protocols, namely, those that can be described by unitary quantum gates acting on arrays of QBs. The main finding of these works is that addressing N QBs at once, by means of a "global entangling operation," can result in a speed-up of the averaged charging power (stored energy over charging time) as compared to charging them individually, in a parallel fashion. As noted in Ref. [24], however, such global entangling operations involve highly nonlocal interactions, which may be difficult to realize in practice.

In this Letter, we propose a practical architecture for a QB constituted by an array of N TLSs (see Fig. 1). We fully relax the constraint on the unitary evolution of the QB employed in previous theoretical works. Such unitary evolution regime occurs only when the dynamics of the energy source is very slow compared to the QB dynamics (i.e., in the Born-Oppenheimer limit). This, although certainly interesting, is motivated more by mathematical convenience than adherence to reality. Here, we consider the more realistic situation in which no time scale separation exists between the QB and energy source subsystems. Accordingly, we treat the system "QB+energy source" in a fully quantum mechanical fashion, which generally results in a nonunitary reduced dynamics of the QB alone. In the proposed architecture, the nonlocal entangling interaction among the N TLSs is achieved by coupling all of them to the same quantum energy source.

Our analysis relies on modeling the array of TLSs, entangled by a common quantized electromagnetic energy source, through the Dicke model [25]; see Fig. 1(b). Interestingly, we find a quantum collective enhancement of the charging power of a factor $\sqrt{N}$, independent of the strength of the TLS-cavity coupling.

Model and charging (discharging) protocol.—We consider the charging process of N TLSs prepared in their ground state $|g\rangle$, via coupling to a single cavity mode residing in the N photon Fock state [26] $|N\rangle$. The initial state of the total system therefore reads

$$|\psi^{(N)}(0)\rangle = |N\rangle \otimes \underbrace{|g, g, \ldots, g\rangle}_{N}. \tag{1}$$

We model the quantum dynamics of the N TLSs coupled to a single cavity mode via the following time-dependent Dicke Hamiltonian [25]

$$\hat{\mathcal{H}}^{(N)}_{\lambda_t} = \hbar\omega_c \hat{a}^\dagger \hat{a} + \omega_a \hat{J}_z + 2\omega_c \lambda_t \hat{J}_x (\hat{a}^\dagger + \hat{a}). \tag{2}$$

Here, $\hat{a}$ ($\hat{a}^\dagger$) annihilates (creates) a cavity photon with frequency ω_c and $\hat{J}_\alpha = (\hbar/2)\sum_i^N \hat{\sigma}_i^\alpha$ with $\alpha = x, y, z$ as the components of a collective spin operator expressed in terms of the Pauli operators $\hat{\sigma}_i^\alpha$ of the ith TLS. The quantity $\hbar\omega_a$ is the energy splitting between the ground $|g\rangle$ and excited state $|e\rangle$ of each TLS. Below, we focus on the resonant regime, $\omega_a = \omega_c$. The strength of the TLS-cavity coupling is given by the dimensionless parameter λ_t, whose explicit dependence on time t specifies the charging (discharging) protocol. For the sake of definiteness, we consider the protocol sketched in Fig. 1(c). (i) The interaction between the TLSs and the cavity is turned on at time $t = 0^+$, $\lambda_{0^+} = \bar{\lambda}$, and kept at this value for $0 < t \leq \tau_c$. During this charging step, energy transfer occurs from the cavity to the array of TLSs. (ii) The interaction is then turned off at time τ_c^+, i.e., $\lambda_{\tau_c^+} = 0$, and kept off for $\tau_c < t \leq \tau_c + \tau_s$. During this storage step, the TLSs are assumed to be isolated from the environment and hence keep their energy. Finally, (iii) the interaction is again turned on for a time τ_d, $\lambda_t = \bar{\lambda}$ for $\tau_c + \tau_s < t \leq \tau_c + \tau_s + \tau_d$. During this discharging step, energy is transferred from the TLSs to the cavity. An alternative protocol, which is fully feasible experimentally [27,32], may rely on a time-independent $\lambda_t \to g$ coupling and a nonzero time-dependent $\Delta_t = \omega_a(t) - \omega_c$ detuning. The equivalence of these two protocols is discussed in Sec. S1 of the Supplemental Material [33].

Parallel charging.—We begin by considering the case in which charging occurs in a parallel fashion; see Fig. 1(a). Namely, we consider N copies of TLSs, each coupled to a distinct cavity. In the case of a single TLS, the Dicke Hamiltonian (2) reduces to the Rabi Hamiltonian [36,37]. The energy $E_{\bar{\lambda}}^{(\|)}(\tau_c)$ stored at time τ_c in a parallel fashion by N copies of such resonant (i.e., $\omega_a = \omega_c$) Rabi QBs is N times the energy $\epsilon_{\bar{\lambda}}(\tau_c)$ stored in a single Rabi QB,

$$E_{\bar{\lambda}}^{(\|)}(\tau_c) = N\epsilon_{\bar{\lambda}}(\tau_c) \equiv \frac{N\hbar\omega_c}{2}[\langle\psi_{\bar{\lambda}}^{(1)}(\tau_c)|\hat{\sigma}_z|\psi_{\bar{\lambda}}^{(1)}(\tau_c)\rangle - \langle\psi^{(1)}(0)|\hat{\sigma}_z|\psi^{(1)}(0)\rangle], \tag{3}$$

with $\hat{\sigma}_z = |e\rangle\langle e| - |g\rangle\langle g|$.

The label $\bar{\lambda}$ in $E_{\bar{\lambda}}^{(\|)}(\tau_c)$ reminds us that the stored energy depends on $\bar{\lambda}$. The symbol $|\psi_{\bar{\lambda}}^{(1)}(\tau_c)\rangle$ stands for the evolved initial state $|\psi^{(1)}(0)\rangle = |1\rangle \otimes |g\rangle$, according to $\hat{\mathcal{H}}_{\bar{\lambda}}^{(1)}$ for a time τ_c, i.e., $|\psi_{\bar{\lambda}}^{(1)}(\tau_c)\rangle = e^{-i\hat{\mathcal{H}}_{\bar{\lambda}}^{(1)}\tau_c/\hbar}|\psi^{(1)}(0)\rangle$.

We now introduce the maximum stored energy (i.e., the "capacity") and charging power in the parallel-charging mode: $E_{\bar{\lambda}}^{(\|)} = \max_{\tau_c}[E_{\bar{\lambda}}^{(\|)}(\tau_c)]$ and $P_{\bar{\lambda}}^{(\|)} = \max_{\tau_c}[P_{\bar{\lambda}}^{(\|)}(\tau_c)]$, where [23,24] $P_{\bar{\lambda}}^{(\|)}(\tau_c) \equiv E_{\bar{\lambda}}^{(\|)}(\tau_c)/\tau_c$.

Both $E_{\bar{\lambda}}^{(\|)}$ and $P_{\bar{\lambda}}^{(\|)}$ scale linearly with N (yielding a constant energy and power per QB): $E_{\bar{\lambda}}^{(\|)} = \hbar\omega_c N\mathcal{F}_E(\bar{\lambda}) \propto N$ and $P_{\bar{\lambda}}^{(\|)} = \hbar\omega_c^2 N\mathcal{F}_P(\bar{\lambda}) \propto N$, where $\mathcal{F}_E(\bar{\lambda})$ and $\mathcal{F}_P(\bar{\lambda})$ are dimensionless functions of $\bar{\lambda}$, which can be calculated exactly [38]. Their expression greatly simplifies in the weak-coupling $\bar{\lambda} \ll 1$ limit, where the Rabi Hamiltonian can be approximated by the Jaynes-Cummings one [39].

The stored energy takes the form $E_{\bar{\lambda}\ll 1}^{(\|)}(\tau_c) \to N\hbar\omega_c \sin^2(\bar{\lambda}\omega_c\tau_c)$, and hence [40] $\mathcal{F}_E(\bar{\lambda} \ll 1) \to 1$ and $\mathcal{F}_P(\bar{\lambda} \ll 1) \to 0.724\bar{\lambda}$. Since we are interested in the collective charging case and in scalings with N, we will not dwell upon deriving exact expressions for $\mathcal{F}_E(\bar{\lambda})$ and $\mathcal{F}_P(\bar{\lambda})$.

Collective charging.—We now investigate the maximum stored energy and maximum charging power when the N TLSs are coupled to the very same cavity [see Fig. 1(b)] as described by Eq. (2). The latter has a conserved quantity given by the so-called cooperation number [41,42] $\hat{J}^2 = \sum_{\alpha=x,y,z}\hat{J}_\alpha^2$. A convenient basis set for representing the Hamiltonian (2) is $|n, j, m\rangle$, where n indicates the number of photons, $j(j+1)$ is the eigenvalue of $\hat{J}^2$, and m denotes the eigenvalue of $\hat{J}_z$. With this notation, the initial state (1) reads $|\psi^{(N)}(0)\rangle = |N, (N/2), -(N/2)\rangle$, while the matrix elements of the Dicke Hamiltonian can be found in Ref. [43] and in Sec. S2 of the Supplemental Material [33].

We remark that the number of photons is not conserved by the Dicke Hamiltonian, nor it is bounded from above, hence taking, in principle, any arbitrarily large integer value. In practice, we need to introduce a cutoff $N_{\rm ph} > N$ on the maximum number $N_{\rm ph}$ of photons. This is chosen in such a way that a larger value of it, $N'_{\rm ph} > N_{\rm ph}$, would not produce any noticeable difference in the computed stored energy. In the following, we show numerical results obtained from an exact numerical diagonalization scheme for $N = 1, \ldots, 20$. We have checked that excellent numerical convergence is achieved by choosing $N_{\rm ph} = 4N$. (A linear scaling of $N_{\rm ph}$ with N has also been found in Ref. [43]).

The energy $E_{\bar{\lambda}}^{(\sharp)}(\tau_c)$ stored collectively at time τ_c by the N TLSs is given by

$$E_{\bar{\lambda}}^{(\sharp)}(\tau_c) = \omega_c[\langle\psi_{\bar{\lambda}}^{(N)}(\tau_c)|\hat{J}_z|\psi_{\bar{\lambda}}^{(N)}(\tau_c)\rangle - \langle\psi^{(N)}(0)|\hat{J}_z|\psi^{(N)}(0)\rangle], \tag{4}$$

where $|\psi_{\bar{\lambda}}^{(N)}(\tau_c)\rangle = e^{-i\hat{\mathcal{H}}_{\bar{\lambda}}^{(N)}\tau_c/\hbar}|\psi^{(N)}(0)\rangle$. The dependence of $E_{\bar{\lambda}}^{(\sharp)}(\tau_c)$ on τ_c is reported in Fig. 2 for a few values of $\bar{\lambda}$. We observe smooth oscillations for $\bar{\lambda} \ll 1$ (red solid line in the inset of Fig. 2), which are in full agreement with results obtained for the Tavis-Cummings model [41,42] (black dotted line in the inset of Fig. 2). In the latter, counter-rotating terms are absent, leading to the conservation of the number of excitations. A more complicated pattern with beatings appears for increasing $\bar{\lambda}$ (green dashed and blue solid lines in Fig. 2).

Figures 3(a) and 3(c) show the maximum stored energy $E_{\bar{\lambda}}^{(\sharp)} \equiv \max_{\tau_c}[E_{\bar{\lambda}}^{(\sharp)}(\tau_c)]$ and charging power $P_{\bar{\lambda}}^{(\sharp)} \equiv \max_{\tau_c}[E_{\bar{\lambda}}^{(\sharp)}(\tau_c)/\tau_c]$ in the collective case, as functions of N, for various values of $\bar{\lambda}$. Note that the vertical axes of Figs. 3(a) and 3(c) are rescaled by N and $\bar{\lambda}N\sqrt{N}$, respectively. We clearly see that such rescaled quantities rapidly converge to an asymptotic value as N increases. This implies that, for sufficiently large values of N, $E_{\bar{\lambda}}^{(\sharp)}$ and $P_{\bar{\lambda}}^{(\sharp)}$ follow the scaling laws

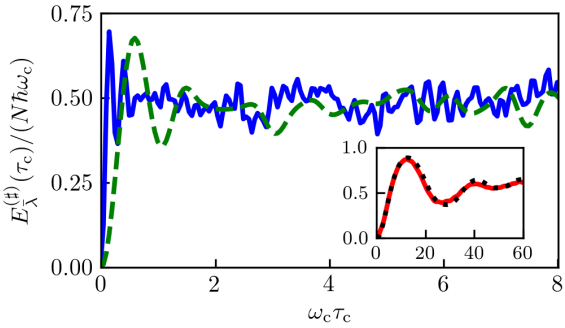

FIG. 2. The dependence of the stored energy $E_{\bar{\lambda}}^{(\sharp)}(\tau_c)$ (in units of $N\hbar\omega_c$) on τ_c (in units of $1/\omega_c$) for $\bar{\lambda} = 0.5$ (green dashed line) and $\bar{\lambda} = 2.0$ (blue solid line). (Inset) Same as in the main panel but for $\bar{\lambda} = 0.05$ (red solid line). Results for the Tavis-Cummings model are denoted by a black dotted line. All shown data have been computed by setting $N = 10$.

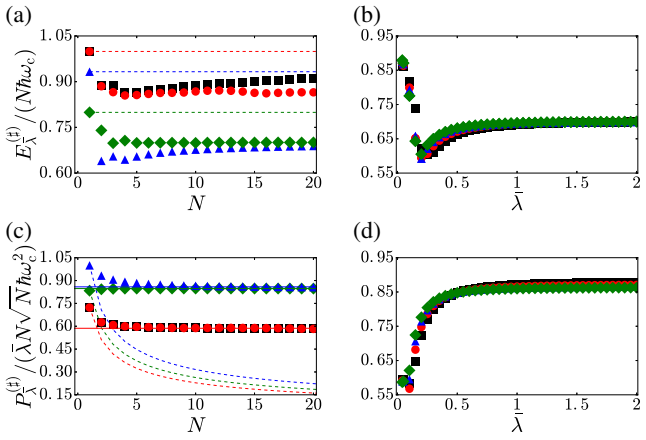

FIG. 3. (a) The maximum stored energy $E_{\bar{\lambda}}^{(\sharp)}$ (in units of $N\hbar\omega_c$) as a function of N. Black squares denote results for the Tavis-Cummings model at $\bar{\lambda} = 0.05$. Results for Dicke QBs refer to $\bar{\lambda} = 0.05$ (red circles), $\bar{\lambda} = 0.5$ (blue triangles), and $\bar{\lambda} = 2.0$ (green diamonds). Dashed lines indicate the values relative to the parallel-charging case. (b) Same as in (a), but as a function of $\bar{\lambda}$ for $N = 6$ (black squares), $N = 8$ (red circles), $N = 10$ (blue triangles), and $N = 12$ (green diamonds). (c) The maximum charging power $P_{\bar{\lambda}}^{(\sharp)}$ (in units of $\bar{\lambda}N\sqrt{N}\hbar\omega_c^2$) as a function of N. Color coding and labeling is the same as in (a). The thin horizontal lines are best fits to the numerical results, indicating the asymptotic values of the maximum power at large N: $\lim_{N\gg 1} P_{\bar{\lambda}}^{(\sharp)}/(\bar{\lambda}N\sqrt{N}\hbar\omega_c^2) = 0.586$ for $\bar{\lambda} = 0.05$ (red), 0.858 for $\bar{\lambda} = 0.5$ (blue), and 0.847 for $\bar{\lambda} = 2$ (green). (d) Same as in (c), but as a function of $\bar{\lambda}$. Color coding and labeling as in (b).

$$E_{\bar{\lambda}}^{(\sharp)} \propto N \tag{5}$$

and

$$P_{\bar{\lambda}}^{(\sharp)} \propto N^{3/2}. \tag{6}$$

The superlinear scaling of the maximum charging power in Eq. (6) constitutes direct evidence of a $\sqrt{N}$ quantum advantage associated with collective charging [24] as compared to parallel charging; see expression for $P_{\bar{\lambda}}^{(\|)}$. Such advantage is related to a scaling law of the time required to reach the maximum power, $\tau_c \propto 1/\sqrt{N}$, and has a quantum mechanical origin. The quantum speed-up is indeed associated with the fact that, unlike in the case of the parallel evolution, the collective evolution proceeds through states characterized by quantum entanglement among the TLSs. Thus, our Dicke QBs clearly display the powerful charging mechanism described in abstract terms in Refs. [23,24]. Finally, Figs. 3(b) and 3(d) illustrate the dependencies of the maximum stored energy and charging power of Dicke QBs on the coupling constant $\bar{\lambda}$, for various values of N. Plotting the same rescaled quantities, $E_{\bar{\lambda}}^{(\sharp)}/(N\hbar\omega_c)$ and $P_{\bar{\lambda}}^{(\sharp)}/(\bar{\lambda}N\sqrt{N}\hbar\omega_c^2)$, versus the effective coupling parameter [44] $\bar{\Lambda} \equiv \bar{\lambda}\sqrt{N}$, one notices a collapse onto universal curves, as shown in Sec. S3 of Ref. [33]. We remind the reader that the ground state of the Dicke model displays a superradiant quantum phase transition (SQPT) at $\bar{\Lambda} = 1/2$. A feeble reminiscence of such SQPT is also seen in the maximum charging energy of Dicke QBs, as illustrated in Sec. S3 of Ref. [33]; see also Ref. [45].

Storage and discharging.—We now briefly comment upon storage and discharging phases of our Dicke QBs. We assume the storage time τ_s is much shorter than any decoherence or relaxation time scale in a real solid-state implementation. Under this assumption, the Dicke QB retains its energy during the storage step. In the parallel case, and when $\bar{\lambda} \ll 1$ (in which case the rotating wave approximation holds), independent of the duration of the storage time τ_s, the initial state (1) is recovered at the end of the discharging phase if the condition $\tau_c + \tau_d = \pi/(\bar{\lambda}\omega_c)$ is met. In the collective case, as either N or $\bar{\lambda}$ increases, such recoverability is lost. Accordingly, the smaller $\bar{\lambda}$ the higher $E_{\bar{\lambda}}^{(\sharp)}$, the higher the recoverability (not shown). This is a signature of energy injection incurred when turning the coupling on and off, namely, that $\delta E_{\bar{\lambda}}^{\mathrm{on}} = \langle \psi_{\bar{\lambda}}^{(N)}(0)|\hat{\mathcal{H}}_{\lambda_{0+}}^{(N)} - \hat{\mathcal{H}}_{\lambda_{0-}}^{(N)}|\psi_{\bar{\lambda}}^{(N)}(0)\rangle$ and $\delta E_{\bar{\lambda}}^{\mathrm{off}} = \langle \psi_{\bar{\lambda}}^{(N)}(\tau_c)|\hat{\mathcal{H}}_{\lambda_{\tau_c+}}^{(N)} - \hat{\mathcal{H}}_{\lambda_{\tau_c-}}^{(N)}|\psi_{\bar{\lambda}}^{(N)}(\tau_c)\rangle$ are generally nonvanishing.

Experimental considerations.—The TLS+cavity system may be realized with state-of-the-art solid-state technology, by using, e.g., superconducting qubits coupled to superconducting line resonators [32,52–54] or nanofabricated quantum dots (see, e.g., Refs. [55,56]) combined with superconductive microwave circuits [56–61], photonic crystals [62], or terahertz planar microcavities [63]. Concerning the typical values of the relevant physical parameters discussed in this Letter, the implementations of Rabi and Dicke Hamiltonians in such solid-state devices [27,32,57] have a resonant frequency $\omega_c \approx \omega_a$ ranging from gigahertz to terahertz values and an individual interaction parameter $g_0 = \bar{\lambda}\omega_c$ typically taking values in the range 10–100 MHz. This leads to $\bar{\lambda} \approx 10^{-3} - 10^{-2}$, which fully justifies the rotating wave approximation discussed for the Rabi model. Moreover, the relevant time scales of relaxation and decoherence processes have to be compared with g_0^{-1}. In particular, one can introduce the decoherence rate Γ_ϕ and the electron relaxation rate Γ_e [8,64]. The proposed charging (discharging) protocol—together with all other possible quantum-computing implementations—is meaningful under the condition $\Gamma_\phi \lesssim \Gamma_e < g_0$, which is satisfied in the experiments discussed in Refs. [27,32,57]. This condition is even further justified in the Dicke model, where the global coupling scales as $g = g_0\sqrt{N}$. Recent experimental work has also demonstrated that the strong-coupling $\bar{\lambda} \approx 1$ limit can also be reached [65–67]. Colloidal quantum dots such as core-shell CdSe dots [68,69] may offer another possible solution for implementing Dicke QBs, bringing the resonant frequency to hundreds of terahertz. This could facilitate the coupling of the dots with the photonic (micro)cavity mode and also yield an improved stored energy density.

Conclusions.—We have introduced the concept of a "Dicke quantum battery," consisting of an array of entangled two-level systems. Our aim is to put on concrete and experimentally feasible grounds the intriguing abstract ideas previously presented in Refs. [23,24]. The main physics is captured by the toy model in Eq. (2), which can in principle be engineered in a solid-state platform and displays collective powerful charging [Eq. (6) and Fig. 3(c)]. In particular, the interaction of an array of two-level systems with a common quantized electromagnetic mode in a cavity automatically creates entanglement among the N two-level systems. This is ultimately due to an effective long-range interaction between the two-level systems mediated by the cavity photons. We observe a $\sqrt{N}$-fold enhanced scaling of the maximum charging power with respect to the parallel case, independent of the value of the coupling strength $\bar{\lambda}$; see Eq. (6). We further note an interesting trade-off between power and reversibility of the charging process. Highest values of the maximum power are achieved at strong coupling. These come, however, at the cost of a lower stored energy, accompanied by a decrease in the efficiency of energy transfer from the quantum batteries to the cavity in the discharging phase. On the other hand, at weak coupling, one finds larger values of

the maximum stored energy and a higher efficiency of energy transfer in the discharging step, at the cost of lower values of the maximum power.

We thank S. Gasparinetti, V. Giovannetti, M. Lewestein, A. Mari, M. Nath Bera, M. Paternostro, F. Pellegrino, and A. Riera for useful discussions. M. C. wishes to thank the COST action MP1209 "Thermodynamics in the Quantum Regime" for support.

*Dario.Ferraro@iit.it

[1] C. A. Vincent and B. Scrosati, *Modern Batteries* (Butterworth-Heinemann, Oxford, 1997).
[2] R. M. Dell and D. A. J. Rand, *Understanding Batteries* (The Royal Society of Chemistry, Cambridge, 2001).
[3] *Advances in Battery Technologies for Electric Vehicles*, edited by B. Scrosati, J. Garche, and W. Tillmetz (Woodhead Publishing, Cambridge, 2015).
[4] X. Luo, J. Wang, M. Dooner, and J. Clarke, Applied Energy **137**, 511 (2015).
[5] G. Wang, L. Zhang, and J. Zhang, Chem. Soc. Rev. **41**, 797 (2012).
[6] S. P. S. Badwal, S. S. Giddey, C. Munnings, A. I. Bhatt, and A. F. Hollenkamp, Front Chem. **2**, 79 (2014).
[7] F. Bonaccorso, L. Colombo, G. Yu, M. Stoller, V. Tozzini, A. C. Ferrari, R. S. Ruoff, and V. Pellegrini, Science **347**, 1246501 (2015).
[8] A. Blais, R.-S. Huang, A. Wallraff, S. M. Girvin, and R. J. Schoelkopf, Phys. Rev. A **69**, 062320 (2004).
[9] M. H. Devoret and R. J. Schoelkopf, Science **339**, 1169 (2013).
[10] D. P. Di Vincenzo, Science **270**, 255 (1995).
[11] S. Vinjanampathy and J. Anders, Contemp. Phys. **57**, 545 (2016).
[12] R. Uzdin, A. Levy, and R. Kosloff, Phys. Rev. X **5**, 031044 (2015).
[13] M. Campisi and R. Fazio, J. Phys. A **49**, 345002 (2016).
[14] B. Karimi and J. P. Pekola, Phys. Rev. B **94**, 184503 (2016).
[15] G. Marchegiani, P. Virtanen, F. Giazotto, and M. Campisi, Phys. Rev. Applied **6**, 054014 (2016).
[16] A. Ü. C. Hardal and Ö. E. Müstecaplioğlu, Sci. Rep. **5**, 12953 (2015).
[17] M. N. Bera, A. Riera, M. Lewenstein, and A. Winter, Nat. Commun. **8**, 2180 (2017).
[18] M. N. Bera, A. Riera, M. Lewenstein, and A. Winter, arXiv:1707.01750.
[19] M. Perarnau-Llobet, H. Wilming, A. Riera, R. Gallego, and J. Eisert, arXiv:1704.05864 [Phys. Rev. Lett. (to be published)].
[20] B. Karimi, J. P. Pekola, M. Campisi, and R. Fazio, Quantum Sci. Technol. **2**, 044007 (2017).
[21] R. Alicki and M. Fannes, Phys. Rev. E **87**, 042123 (2013).
[22] K. V. Hovhannisyan, M. Perarnau-Llobet, M. Huber, and A. Acín, Phys. Rev. Lett. **111**, 240401 (2013).
[23] F. C. Binder, S. Vinjanampathy, K. Modi, and J. Goold, New J. Phys. **17**, 075015 (2015).
[24] F. Campaioli, F. A. Pollock, F. C. Binder, L. Céleri, J. Goold, S. Vinjanampathy, and K. Modi, Phys. Rev. Lett. **118**, 150601 (2017).
[25] R. H. Dicke, Phys. Rev. **93**, 99 (1954).
[26] Experimentally, the preparation of quantum systems in Fock states for small N has been demonstrated, e.g., in Refs. [27–31]. We have checked in a number of exactly solvable models of QBs—not shown here—that the quantum collective enhancement of the maximum charging power, scaling like $\sqrt{N}$ for $N \gg 1$, does not depend on the choice of the initial state for the cavity photons and does not occur only for Fock states, but also for coherent as well as thermal states; G. M. Andolina *et al.* (to be published).
[27] M. Hofheinz, E. M. Weig, M. Ansmann, R. C. Bialczak, E. Lucero, M. Neeley, A. D. O'Connell, H. Wang, J. M. Martinis, and A. N. Cleland, Nature (London) **454**, 310 (2008).
[28] M. Hofheinz, H. Wang, M. Ansmann, R. C. Bialczak, Erik Lucero, M. Neeley, A. D. O'Connell, D. Sank, J. Wenner, J. M. Martinis, and A. N. Cleland, Nature (London) **459**, 546 (2009).
[29] R. W. Heeres, B. Vlastakis, E. Holland, S. Krastanov, V. V. Albert, L. Frunzio, L. Jiang, and R. J. Schoelkopf, Phys. Rev. Lett. **115**, 137002 (2015).
[30] S. Gasparinetti, S. Berger, A. A. Abdumalikov, M. Pechal, S. Filipp, and A. J. Wallraff, Sci. Adv. **2**, e1501732 (2016).
[31] S. P. Premaratne, F. C. Wellstood, and B. S. Palmer, Nat. Commun. **8**, 14148 (2017).
[32] J. M. Fink, R. Bianchetti, M. Baur, M. Göppl, L. Steffen, S. Filipp, P. J. Leek, A. Blais, and A. Wallraff, Phys. Rev. Lett. **103**, 083601 (2009).
[33] See Supplemental Material at http://link.aps.org/supplemental/10.1103/PhysRevLett.120.117702 for additional information. It is divided into four Sections: S1. Consideration on an alternative charging (discharging) protocol, S2. Matrix elements of the Dicke Hamiltonian, S3. Universality, S4. On the role of a quadratic term in the photonic field, which includes [8,34,35].
[34] W. P. Schleich, *Quantum Optics in Phase Space* (Wiley, Berlin, 2001).
[35] A. B. Klimov and S. M. Chumakov, *A Group-Theoretical Approach to Quantum Optics* (Wiley, Weinheim, 2009).
[36] I. I. Rabi, Phys. Rev. **49**, 324 (1936).
[37] I. I. Rabi, Phys. Rev. **51**, 652 (1937).
[38] D. Braak, Phys. Rev. Lett. **107**, 100401 (2011).
[39] E. T. Jaynes and F. W. Cummings, Proc. IEEE **51**, 89 (1963).
[40] The prefactors can be understood considering the fact that $y = 1 - \cos x$ has absolute maximum $y_{\max} = 2$ at $x_{\max} = \pi$ (mod $[2\pi]$), while $y = (1 - \cos x)/x$ has the absolute maximum $y_{\max} \approx 0.724$ at $x_{\max} \approx 2.331$, as can be easily achieved by numerical investigation.
[41] M. Tavis and F. W. Cummings, Phys. Rev. **170**, 379 (1968).
[42] M. Tavis and F. W. Cummings, Phys. Rev. **188**, 692 (1969).
[43] M. A. Bastarrachea-Magnani and J. G. Hirsch, Rev. Mex. Fis. S **57**, 69 (2011).
[44] C. Emary and T. Brandes, Phys. Rev. E **67**, 066203 (2003).
[45] We note that the possibility to achieve a SQPT in a real solid-state device has been debated at length [46–51]. This is due to the detrimental effect of a term quadratic in the

bosonic field, i.e., $\propto (\hat{a}^\dagger + \hat{a})^2$, which is missing in Eq. (2) and typically emerges from the minimal coupling of matter with the cavity radiation field. The authors of Refs. [47,49] have argued, however, that this term does not prevent the emergence of SQPTs in alternative artificial TLSs such as phase qubits. We have investigated the role of the $(\hat{a}^\dagger + \hat{a})^2$ term and found it to be irrelevant with respect to our main findings above. For details, see Sec. S4 of Ref. [33].

[46] G. Chen, Z. Chen, and J. Liang, Phys. Rev. A **76**, 055803 (2007).
[47] P. Nataf and C. Ciuti, Phys. Rev. Lett. **104**, 023601 (2010).
[48] P. Nataf and C. Ciuti, Nat. Commun. **1**, 72 (2010).
[49] O. Viehmann, J. von Delft, and F. Marquardt, Phys. Rev. Lett. **107**, 113602 (2011).
[50] L. Chirolli, M. Polini, V. Giovannetti, and A. H. MacDonald, Phys. Rev. Lett. **109**, 267404 (2012).
[51] F. M. D. Pellegrino, L. Chirolli, R. Fazio, V. Giovannetti, and M. Polini, Phys. Rev. B **89**, 165406 (2014).
[52] J. Clarke and F. K. Wilhelm, Nature (London) **453**, 1031 (2008).
[53] A. Wallraff, D. I. Schuster, A. Blais, L. Frunzio, R.-S. Huang, J. Majer, S. Kumar, S. M. Girvin, and R. J. Schoelkopf, Nature (London) **431**, 162 (2004).
[54] Z.-L. Xiang, S. Ashhab, J. Q. You, and F. Nori, Rev. Mod. Phys. **85**, 623 (2013).
[55] A. Singha, M. Gibertini, B. Karmakar, S. Yuan, M. Polini, G. Vignale, M. I. Katsnelson, A. Pinczuk, L. N. Pfeiffer, K. W. West, and V. Pellegrini, Science **332**, 1176 (2011).
[56] T. Hensgens, T. Fujita, L. Janssen, X. Li, C. J. Van Diepen, C. Reichl, W. Wegscheider, S. Das Sarma, and L. M. K. Vandersypen, Nature (London) **548**, 70 (2017).
[57] A. Stockklauser, P. Scarlino, J. V. Koski, S. Gasparinetti, C. K. Andersen, C. Reichl, W. Wegscheider, T. Ihn, K. Ensslin, and A. Wallraff, Phys. Rev. X **7**, 011030 (2017).
[58] B. Küng, C. Rössler, M. Beck, M. Marthaler, D. S. Golubev, Y. Utsumi, T. Ihn, and K. Ensslin, Phys. Rev. X **2**, 011001 (2012).
[59] J. Basset, D.-D. Jarausch, A. Stockklauser, T. Frey, C. Reichl, W. Wegscheider, T. M. Ihn, K. Ensslin, and A. Wallraff, Phys. Rev. B **88**, 125312 (2013).
[60] C. Rössler, D. Oehri, O. Zilberberg, G. Blatter, M. Karalic, J. Pijnenburg, A. Hofmann, T. Ihn, K. Ensslin, C. Reichl, and W. Wegscheider, Phys. Rev. Lett. **115**, 166603 (2015).
[61] A. Hofmann, V. F. Maisi, C. Rossler, J. Basset, T. Krähenmann, P. Märki, T. Ihn, K. Ensslin, C. Reichl, and W. Wegscheider, Phys. Rev. B **93**, 035425 (2016).
[62] Y. Ben, Z. Hao, C. Sun, F. Ren, N. Tan, and Y. Luo, Opt. Express **12**, 5146 (2004).
[63] Q. Zhang, M. Lou, X. Li, J. L. Reno, W. Pan, J. D. Watson, M. J. Manfra, and J. Kono, Nat. Phys. **12**, 1005 (2016).
[64] R. J. Schoelkopf and S. M. Girvin, Nature (London) **451**, 664 (2008).
[65] F. Yoshihara, T. Fuse, S. Ashhab, K. Kakuyanagi, S. Saito, and K. Semba, Nat. Phys. **13**, 44 (2017).
[66] N. K. Langford, R. Sagastizabal, M. Kounalakis, C. Dickel, A. Bruno, F. Luthi, D. J. Thoen, A. Endo, and L. DiCarlo, Nat. Commun. **8**, 1715 (2017).
[67] J. Braumüller, M. Marthaler, A. Schneider, A. Stehli, H. Rotzinger, M. Weides, and A. V. Ustinov, Nat. Commun. **8**, 779 (2017).
[68] A. Comin and L. Manna, Chem. Soc. Rev. **43**, 3957 (2014).
[69] L. De Trizio and L. Manna, Chem. Rev. **116**, 10852 (2016).